OCDM System with PAPR Reduction for Sub-THz Wireless Communication

Md. Moklesur Rahman, Heung-Gyoon Ryu
Department of Electronic Engineering
Chungbuk National University,
Cheongju 28644, Korea
m.moklesur.r@gmail.com, ecomm@cbu.ac.kr

***Abstract* – Next-generation wireless technology which will use Sub-THz frequency band will support several new services and applications. However, there is a very high propagation loss of communication signals in Sub-THz frequency band. Furthermore, the power efficiency will be greatly decreased because of the high peak-to-average power ratio (PAPR) in the multi-carrier communication signal. As a result, PAPR reduction is the most important in 6G wireless communication system than 4G long-term evolution (LTE), 5G new radio (NR) schemes because it will use the Sub-THz frequency band of very high propagation loss. Therefore, spread spectrum technology termed as orthogonal chirp division multiplexing (OCDM) takes into account for the orthogonality of cyclically shifted quadratic chirp signals in order to increase the spectral efficiency and reduce the propagation loss. In this paper, we suggest a new discrete Fourier transform (DFT)-Spread OCDM (DFT-Spread OCDM) system for designing waveform and suitably acceptable PAPR reduction. Comparing the proposed scheme to the conventional OFDM and OCDM systems, simulation findings show that this technique greatly reduces PAPR by about 2 dB. Additionally, we examine the bit error ratio (BER) performance in AWGN channel. This DFT-Spread OCDM scheme performs almost similar results as compared to the previous OFDM and OCDM systems.**

Keywords* – *OCDM,* Wireless communication, 6G, *Sub-THz, DFT-Spread, PAPR, power efficiency.

I. INTRODUCTION

Orthogonal frequency division multiplexing (OFDM) scheme is the one that is most frequently used in recent wireless communication systems. It is currently an essential component of 5G networks and was used in the long-term evolution (LTE) standard [1]. This is frequently used due to its straightforward implementation, the availability of equalization techniques, lack of complexity, and its resistance to multi-path fading. As consequence, there has been a strong drive among physical layer scientists to investigate the next generation technology as the future wireless networks which will experience higher traffic volumes and minimum interference abidance [2-4]. But the propagation loss, out-of-band (OOB) power emission and narrow band interference (NBI) issues have a major negative influence on the average performance [5-7]. As a result, upcoming wireless communication systems like 6G, the OCDM waveform can be a better substitute of OFDM, or filter bank-based modulations. In contrast to sinusoids, chirps in OCDM actually carry the data symbols [8].

Moreover, the OFDM modulations are only marginally effective on channels that are selective in the time domain but chirp multiplexing enables the receiver to decode the signal that are selective in the time and frequency domains [9]. The OCDM system, however, has a high peak-to-average power ratio (PAPR) similar to the OFDM system due to the increasing number of OCDM symbols. The optimum PAPR signals compel power amplifiers to perform mostly in the non-linear region which results in non-linear distortion. This non-linearity of high power amplifier creates in-band distortion, as a result bit error rate (BER) and OOB power increases, and introduces adjacent channel interference (ACI). In order to increase the effectiveness of uplink transmission and decreasing propagation loss, a PAPR reduction technique for OCDM system based on the discrete Fourier transform (DFT) precoding process is presented in this study. To efficiently minimize the PAPR of the system, DFT precoding is performed prior to inverse discrete Fresnel transform (IDFnT) operation at the transmitter side [10]. As opposed to the Fourier transform utilized in OFDM, the Fresnel transform be the foundation of OCDM modulation. Even yet, it is demonstrated that the OCDM modulation can be handled using a standard inverse discrete Fourier Transform (IDFT) by chirp multiplication both in the frequency and time domains, both before and after, thereby simplifying the transceiver in comparison to the Fresnel transform [11-12].

In this paper, we suggest a new spectrum efficient waveform candidate using DFT-Spread OCDM for sub-THz wireless communications system like 6G services. By implementing the DFT-Spread, it is possible to reduce PAPR significantly without sacrificing such communication quality. The suggested scheme can impressively reduce the PAPR by 2 dB as compared to the conventional OFDM and OCDM systems respectively. The BER performances using AWGN channel of OFDM, OCDM, DFT-Spread systems are also analyzed in this paper.

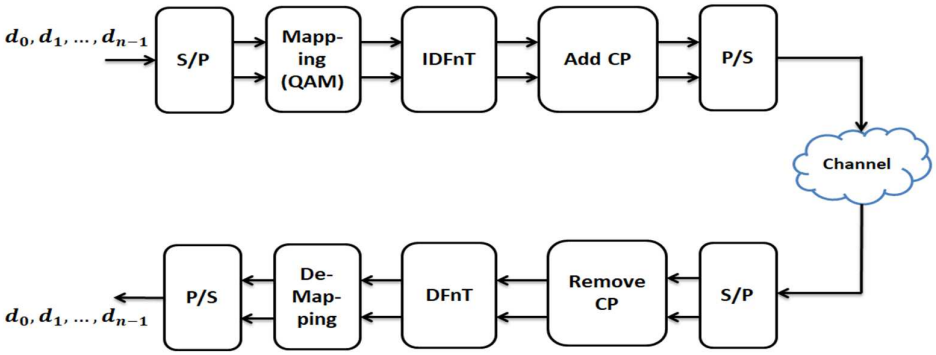

Fig.1. Transmitter and receiver block diagram of conventional OCDM system.

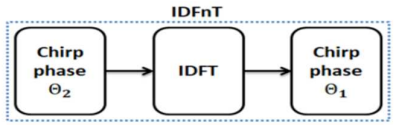

(a)

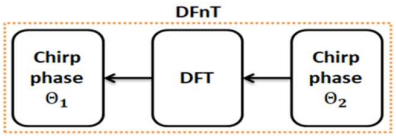

(b)

Fig. 2. Generation of IDFnT from IDFT.

II. OCDM SYSTEM

Fig. 1 illustrates a block diagram of the conventional OCDM system's framework. The system is just like an OFDM scheme except Fresnel transform used instead of FFT. The optical field coefficients of the Talbot image, also known as self-image, are provided by the DFnT matrix at the prediction of Talbot distance, $D_T = \frac{Z_T}{N}$, where $Z_T = \frac{d^2}{\lambda}$; d be the separation between successive gratings. The DFnT is formulated in earlier studies to describe the factors of Talbot image. The DFnT matrices exhibit degeneracy in two ways as, if N is even, they have a size of N/2, but if N is odd, they have a size of N. The use of DFnT as a general mathematical tool is constrained by this degeneracy. In recent work, OCDM system transmits data bits by encoding and then mapped by a complex modulation technique. The effects of utilizing a higher order constellation have been thoroughly studied, hence in this study we just take into account 4-QAM. The IDFnT may then perform the synthesis process to be discretized modulated chirp signals. For stacking the symbols into the perfect vector form, we can define a compact matrix form as $x(i) = [x(iN), x(iN+1), \ldots, x(iN+N-1)]^T$, thus the discrete OCDM signal is defined by [8]

symbols can then be obtained by carrying out the reverse operation i. e DFnT. As a result, restored symbols will be $x'(i) = \phi S(i) = x(i)$. Now, (m, n)-th component of N × N DFnT matrix of ϕ can be expressed as [9-10]

$$\phi(m,n) = \frac{1}{N} e^{-j\frac{\pi}{4}} \times \begin{cases} e^{j\frac{\pi}{n}(m-n)^2}; & N = 0\ (mod\ 2) \\ e^{j\frac{\pi}{N}(m+0.5-n)^2}; & N = 1\ (mod\ 2) \end{cases} \quad (2)$$

The Fresnel transform with the help of Eq. (2) constitutes DFnT using additional quadratic phases Θ_1 and Θ_2. Afterword, the relation can be used to decompose the DFnT matrix as $\phi = \Theta_1 \mathcal{F} \Theta_2$. The supplementary exponential phases in discrete form of diagonal matrices are given by [10]

$$\Theta_1 = e^{j\pi/4} \times \begin{cases} e^{j\pi m^2/N} & N = 0; \quad (mode\ 2) \\ e^{j\pi/4N} e^{j\pi/N(m^2+m)} & N = 1\ ; (mode\ 2) \end{cases}$$
$$\Theta_2 = e^{j\pi/4} \times \begin{cases} e^{j\pi n^2/N} & N = 0; \quad (mode\ 2) \\ e^{j\pi/N(n^2-n)} & N = 1\ ; (mode\ 2) \end{cases} \quad (2)$$

The n^{th} element modulated symbol is given by dropping the block index and applying Eq. (2) [9].

$$s(n) = e^{j\frac{\pi}{4}} \sum_{k=0}^{N-1} x(k) e^{j\frac{\pi}{N}(n-k)^2} \quad (3)$$

Adding CP of length, N_{CP}, the resulting block is created. After that the continuous-time interpolated signal is then expressed as [8]

$$s'(t) = \begin{cases} s(t + T_s - T_{CP}); & 0 \le t < T_{CP} \\ s(t - T_{CP}); & T_g \le t < T_s + T_{CP} \end{cases} \quad (4)$$

where $T_{CP} = N_{CP} T_s / N$ is the CP duration. Before defining s(t), we should introduce continuous-time chirp signal as

$$\Psi_0(t) = e^{j\frac{\pi}{4}} e^{-j\pi\frac{N}{T_s^2}t^2}; \qquad 0 \le t < T_s \quad (5)$$

As demonstrated in [9], the periodically extended continuous signal produced by interpolating the discrete samples, provided by

$$s(t) = \sum_{k=0}^{N-1} x(k)\Psi_0\left(t - \frac{kT_s}{N}\right)\prod_T(t) \quad (6)$$

here $\prod_T(t) = 1$ if $0 \le t < T$ and 0 otherwise. Generally, the spectral bandwidth of each chirp signal is B. Every spectrum of $\Psi_k(t)$ into the baseband form is being folded within $-B/2$ and $B/2$. Finally, in the receiver section, information signal be down converted to baseband and then filtered as it was being received to have the expected information signal

$$y(t) = e^{j2\pi\Delta_f t}\int h(t,\tau)s'(t-\tau)d\tau + \nu(t) \quad (7)$$

where τ denotes the tap delay, $h(t,\tau)$ is the aggregate channel impact, Δ_f denotes the carrier frequency offset resulting from oscillator mismatch or phase noise, and $\nu(t)$ is the white additive Gaussian noise (AWGN).

III. DFT-Spread OCDM System

The suggested DFT-Spread OCDM system illustrated in Fig. 3, the digital modulator (i.e., QAM) transforms the synthetically produced binary input data into a series of complex-valued hierarchical modulation symbol $x_m(m = 0, 1, 2, \dots, M-1)$. Complex data symbols are converted from serial-to-parallel (S/P) streams via the S/P module. One of the most essential aspects of wireless communication networks is to make lower PAPR, particularly for the effective uplink transmissions. To reduce the transmitted signal's PAPR, DFT $[X_k(k = 0, 1, 2, \dots, M-1)]$ precoding is employed. The DFT is applied to an individual block of x_m at the transmitter section prior to the IDFnT. The PAPR of OCDM signal must be examined after the OCDM operation performed, in which the OCDM modulator changes the time- frequency signal from the IDFnT block to the time-domain signal as shown in Fig. 3. The transformation of IDFT to IDFnT is also illustrated in Fig. 2.

Therefore, the OCDM signal's PAPR can be expressed as [2-4]

$$\text{PAPR}\{s(t)\} = \frac{max[|s(t)|^2]}{E[|s(t)|^2]} \quad (8)$$

where max (.) represents max value function and E[.] is the expected value of $[|s(t)|^2]$. But the OCDM symbols can be approximated by normal random variables, the CCDF of OCDM system is defined as the probability that the PAPR of the transmit symbols surpasses a threshold value ϒ, and mathematically expressed as

$$\Pr(\text{PAPR}>\Upsilon) = 1 - [1 - e^{-\gamma}]^N \quad (9)$$

where Pr(.) represents the probability function. A sampling rate of N/T_s and an L-times oversampling can produce the discrete-time characterization where L = 4 is the oversampling factor we used in this investigation. A supplementary signal processing stage on the transmitter side conducts M-point DFT precoding to an individual block of symbol after mapping it onto each subcarrier. The PAPR of the transmitted signal is constrained by means of this DFT precoding. As an example, during N=32 and DFT size M=4, the subband numbers will be 32/4 or 8. When subbands are changed, the PAPR varies depending on the DFT size used to represent the frequency-domain samples.

IV. Simulation Results

The simulation results of the suggested DFT-Spread WR-OCDM scheme are represented in this section by comparing with the conventional OFDM and OCDM systems. We use 4-QAM modulation with N= 1024 subcarriers, DFT size M=256, 256 OCDM symbols, and sampling frequency = 80 MHz throughout the simulations. This sampling frequency is used of the simulation scheme as an example for MHZ/GHz applications. AWGN is considered to evaluate the proposed system. We take into account the performances of power spectral density (PSD), PAPR and BER for each system as figures of merit. The list of simulation parameters are demonstrated in Table 1.

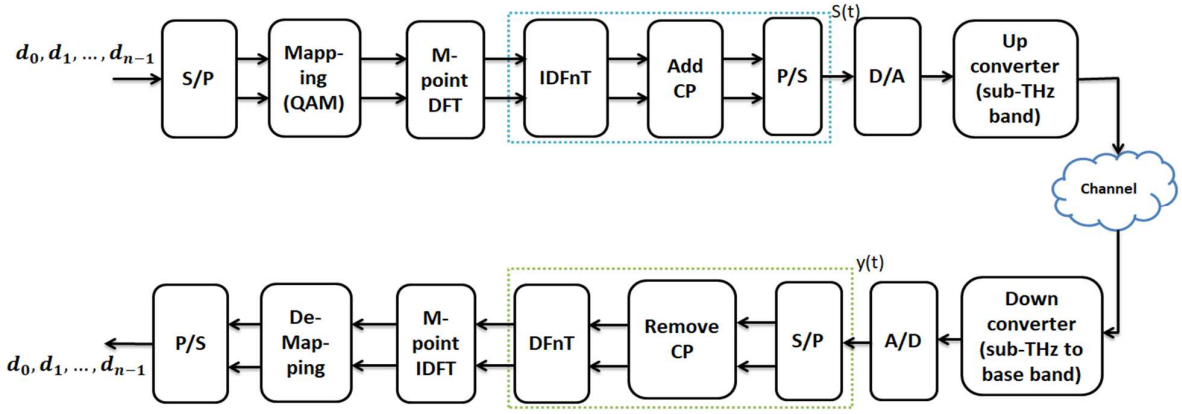

Fig. 3. DFT-Spread OCDM system for sub-THz communications.

The power spectra during 80 MHz frequency of OFDM and OCDM schemes are presented in Fig. 5. Instead of taking MHz sampling frequency, it could be used GHz frequency band as the sampling frequency for sub-THz band applications. It is noticed that the PSD of the OCDM module is not equivalent to that of OFDM. The OCDM scheme achieves -41.256 dB OOB power whereas the OFDM system exhibits as -46 dB. Fig. 5 represents the PAPR performance of OCDM scheme for different modulation orders. This illustrates a comparative analysis of PAPR between the suggested DFT-Spread OCDM scheme and the conventional systems. However, the PAPR reduction performance of DFT-Spread OCDM scheme due to the CCDF level of 10^{-3} exhibited as about 2 dB lower compared to OFDM and OCDM systems. Using 4-QAM signaling and AWGN channel, the BER performance of OFDM, OCDM and new DFT-Spread OCDM system depicted in Fig. 6. This graph illustrates that the BER evaluation of the proposed method is exactly equivalent to the OFDM and OCDM schemes.

Table 1. Simulation Parameters

Parameters	**Values**
Modulation alphabet	4-QAM
No. of subcarriers , N	1024
DFT size, M	256
No. of chirps	256
CP length	(1/8)*N
Sampling frequency	80 MHz
Chirp signal frequency	(1-400) Hz
Channel	AWGN

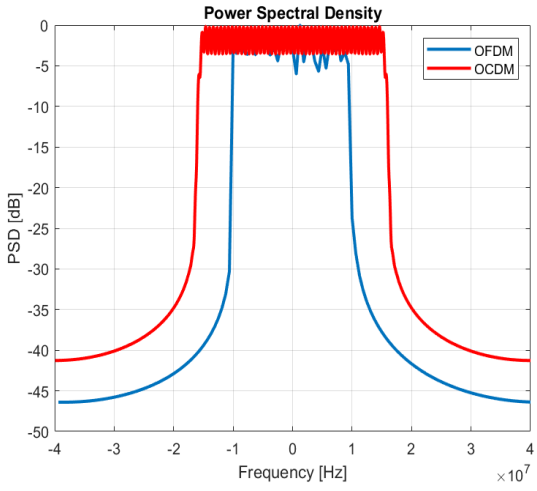

Fig. 4. Example power spectrum of the OFDM and OCDM schemes during 80 MHz smapling frequency.

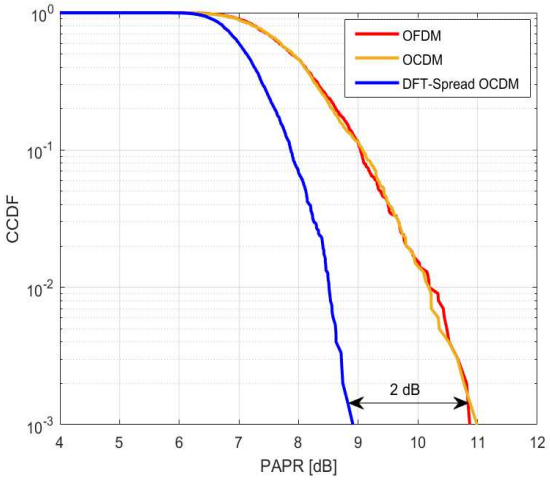

Fig. 5. CCDF comparison of PAPR performance for different systems.

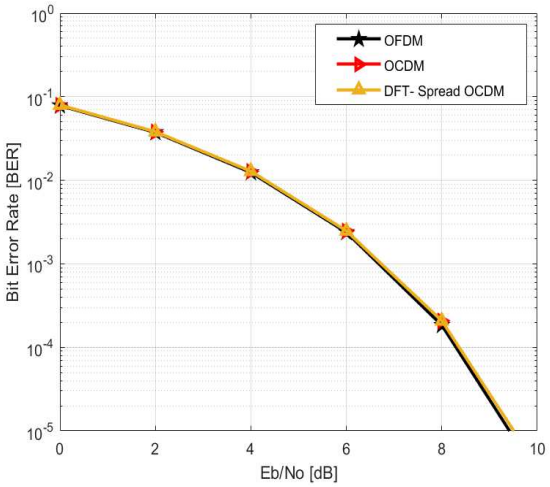

Fig. 6. BER performance of OFDM, OCDM and DFT-Spread OCDM systems.

V. Conclusions

This paper incorporates with the design of DFT-Spread OCDM scheme as a unique PHY layer attractive waveform candidate in order to achieve higher spectrum efficiency for B5G and 6G wireless communication systems. The suggested system is a straightforward and easily adapted with the conventional OFDM and OCDM systems with a minimal level of complexity. The simulation findings depict that the DFT- Spread OCDM system exhibits equivalent BER performance over AWGN and can effectively achieve lower PAPR value. Finally, it is demonstrated that the suggested scheme can minimize the PAPR about 2 dB in comparison to the existing OFDM and OCDM systems.

References

[1] A. Basireddy and H. Moradi, OFDM Waveform Design for Interference Resistant Automotive Radars, IEEE Sensors Journal, vol. 21, pp. 15670-15678, 2021.

[2] Y. Huleihel, E. Ben-Dror and H. H. Permuter, Low PAPR Waveform Design for OFDM Systems Based on Convolutional Autoencoder, IEEE International Conference on ANTS, New Delhi, India, pp. 1-6, 2020.
[3] Al-Jawhar, Y.A., Ramli, K.N., Taher, et al., “Improving PAPR performance of filtered OFDM for 5G communications using PTS,” ETRI Journal, vol. 43, pp. 209-220, 2021.
[4] M. N. Hossain, T. Shimamura, H. -G. Ryu, et al., “Waveform Design of DFT-Spread WR-OFDM System for the OOB and PAPR Reduction,” ICTC, Jeju, Korea (South), pp.792-796, 2018.
[5] M. Jasim Mohammed, A. A. Kareem, “Prototype filter design for filter bank multicarrier modulation,” J. of Phys. Conf. Ser. Vol. 1973, pp. 012098, 2021
[6] S. A. Matin and L. B. Milstein, "OFDM System Performance, Variability and Optimality With Design Imperfections and Channel Impediments," IEEE Transactions on Vehicular Technology, vol. 70,pp. 381-397, 2021
[7] M. N. Hossain, Y. Sugiura, H. -G. Ryu, et al., “Waveform Design of Low Complexity WR-OTFS System for the OOB Power Reduction,” IEEE Wireless Communications and Networking Conference Workshops, Seoul, Korea (South), pp. 1-5, 2010.
[8] X. Ouyang and J. Zhao, “Orthogonal chirp division multiplexing,” IEEE Transactions on Communications, vol. 64, pp. 3946–3957, 2016.
[9] M. S. Omar and X. Ma, “Performance Analysis of OCDM for Wireless Communications,” IEEE Transactions on Wireless Communications, vol.20, pp. 4032-4043, 2021.
[10] M. S. Omar and X. Ma, “Spectrum Design for Orthogonal Chirp Division Multiplexing Transmissions,” IEEE Wireless Communications Letters, vol. 9, pp. 1990-1994, 2020.
[11] X. Ouyang, O. A. Dobre, Y. L. Guan, et al., “Chirp Spread Spectrum Toward the Nyquist Signaling Rate—Orthogonality Condition and Applications,” IEEE Signal Processing Letters, vol. 24, pp. 1488-1492, 2021.
[12] T. M. Pham, A. N. Barreto, G. P. Fettweis, “Efficient Communications for Overlapped Chirp-Based Systems,” IEEE Wireless Communications Letters, vol. 9, pp. 2202-2206, 2020.